



## Adsorption of Polyelectrolyte Layers of polyethyleneimine and poly(sodium 4-styrene sulfonate) on silver nanoparticles surface: A hue changing study

**\*Muhammaad Taqiyuddin Mawardi, Ayob**

School of Applied Physics, Faculty of Science & Technology, The National University of Malaysia, 43600 Bangi, Selangor, Malaysia, \*Corresponding Author

**Irman, Abdul Rahman**

School of Applied Physics, Faculty of Science & Technology, The National University of Malaysia, 43600 Bangi, Selangor, Malaysia

**Christopher, Gibson**

Flinders Centre for NanoScale Science & Technology (CNST), School of Chemical & Physical Sciences, Flinders University, 5042 South Australia, Australia

**Zainovia, Lockman**

School of Materials and Mineral Resources Engineering, Universiti Sains Malaysia, 14300 Nibong Tebal, Seberang Perai Selatan, Pulau Pinang, Malaysia.

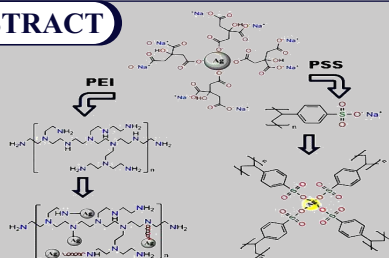
**Shahidan, Radiman**

School of Applied Physics, Faculty of Science & Technology, The National University of Malaysia, 43600 Bangi, Selangor, Malaysia

**David, Lewis**

Flinders Centre for NanoScale Science & Technology (CNST), School of Chemical & Physical Sciences, Flinders University, 5042 South Australia, Australia

### ABSTRACT



The current study report the effects of the addition of 0.1, 0.5, 1.0, 1.5 and 2.0 wt.% protic polyethyleneimine and aprotic poly(sodium 4-styrene sulfonate) polymers in producing different colors of AgNPs solution. The kinetic study was monitored by time-dependent surface plasmon resonance bands in the UV-vis region and by analysing the data obtained from absorption peaks of UV-vis spectra. The results revealed that a wide range of colors can be perfectly tuned by means of fine control of the polyethyleneimine and poly(sodium 4-styrene sulfonate) concentrations. The possible mechanisms that contributed to the changing of AgNP's color are proposed.

**KEYWORDS :** thymomas; thymic carcinomas; prognostic; multimodal management; postoperative radiotherapy; toxicity.

### Introduction:

Nowadays, nanoparticles provide a unique and useful opportunity for a great potential application in medical,<sup>1</sup> optical,<sup>2</sup> or electronic devices such as solar energy panel,<sup>3</sup> drug targetry system,<sup>4</sup> optical sensor<sup>5</sup> and so forth due to their special characteristics of high surface to volume ratio and nanometric size. Among those nanoparticles, silver have recently attracted great attention because it has strong optical absorption in the visible region due to localized surface plasmon resonance (LSPR) of free electrons which can be tuned by controlling the particles size and shape,<sup>6</sup> enabling the monitoring of their evolution and color formation by UV-Vis measurements. Moreover, biomedical advancement using silver nanoparticles (AgNPs) are interesting topic to be explored as AgNPs have continually been used for both biomedical<sup>7</sup> and imaging applications.<sup>8</sup> However, the instability of nanoparticles gives rise to aggregation which deters its use for specific applications. The surface charge and color solution of AgNPs, an essential desired feature remains a key challenge. There are ways to overcome these using surface modification treatments such as citrate,<sup>9</sup> chitosan,<sup>10</sup> silanization<sup>11</sup> and polymer<sup>12</sup> coating through steric or depletion stabilization. Besides, polymer coatings have been found to protect AgNPs and more suitable in bio-related labelling applications.<sup>7</sup> Therefore, the interest in surface treatment or coating is on interpretation of combination of the properties of two or more materials involved with the emphasis on the fact that one of the materials (shell) will determine the surface properties of the particle while the other i.e. the core is completely encapsulated by the shell.

In this study, we report the preparation of AgNPs from aqueous solutions of Ag<sup>+</sup> salts by chemical reduction at room temperature using citrate as protecting agent and focus more on modified AgNPs surface with a protic polyethyleneimine (PEI) and aprotic poly(sodium 4-styrene sulfonate) (PSS) polymers producing different colors of AgNPs solution within coatings on the surface of AgNPs to provide

steric hindrance for colloidal stability. PEI and PSS polymers with different functional groups were chosen for inorganic-organic complexes such that nanocomposite complexes formation could be compared. PEI is a branched chain polymer with a ratio of 1:2:1 for primary: tertiary amine groups and two carbons aliphatic CH<sub>2</sub>CH<sub>2</sub> spacer. Apart from improves AgNPs colloidal stability, AgNPs-capped PEI are also attracting researcher's attention due to its antimicrobial activity.<sup>13</sup> Besides, PSS was chosen because of their antimicrobial for the prevention of sexually transmitted diseases<sup>14</sup> or as proton exchange membranes in fuel cell applications.<sup>15</sup> PSS is also a branched chain polymer contains phenyl and sulfonate functional group with a strong anionic polyelectrolyte, possessing a number of negative charges along its backbone chain which directly replaces citrate shell from AgNPs core, forming intermediate charged clusters. Due to this, PEI and PSS are of special interest because it can control and stabilize both AgNPs and clusters along the polymeric chains with a high stability with time.

It was found that the polymers formed by coatings absorbed polymers on AgNPs from aggregation within solution and remains stable for months. Another part from this study is to demonstrate the formation of colloidal complexes resulting from the spontaneous association of AgNPs and polymers functional groups that could changes or reduces its sols' color. We observed enthalpy-driven binding involving electrostatic interactions and adsorption mechanisms between silver particles and polymers. The AgNPs- polymer complexes thus formed were characterized using UV-Vis, dynamic light scattering (DLS), Fourier transform infrared (FTIR), Raman spectroscopy, scanning electron microscopy (SEM) and transmission electron microscopy (TEM). To our knowledge, this is the first time that an experimental study based on the influence of PSS and PEI molar concentrations to obtain varying colors of silver nanoparticles sols has been reported in the literature.

## Experimental:

### Synthesis of silver nanoparticles

Five portions of each polyethyleneimine (average  $M_w=750k$ ) and poly(sodium 4-styrene sulfonate) (average  $M_w=70k$ ) of 0.1, 0.5, 1.0, 1.5 and 2.0 wt.% stock solutions were made by dissolving 0.02, 0.1, 0.2, 0.3 and 0.4 g of each polymer in 20 mL deionised water at room temperature, respectively. The solutions were magnetically stirred for one hour. Meanwhile, aqueous mixtures of silver nitrate ( $AgNO_3$ , 0.375 mM, 120 mL), trisodium citrate ( $Na_3C_6H_5O_7$ , 12.5 mM, 48 mL) and hydrogen peroxide ( $H_2O_2$ , 50 mM, 120 mL) were prepared. The bulk sample was divided into two parts and a potassium bromide solution (KBr, 1 mM; 180 & 360  $\mu$ L) was added to each solution described above and stirred another one hour to make different sizes of AgNPs, respectively. Subsequently, sodium borohydride ( $NaBH_4$ , 5 mM, 25-30 mL) was injected to each mixed solution and the reaction was initiated. The stirring was continued for another 1 hr to complete their reaction. The different color of solution products confirms the formation of silver nanoparticles with different sizes.<sup>16</sup> The synthesized AgNPs dispersions showed no changes in the position of their optical absorption bands and intensity even after two months of storage at room conditions. A large quantity of such solution was made and served as the stock solution for AgNPs/polymer hue changing studies.

### Coating of AgNPs by Polymers

Polymeric composites of Ag-PEI and Ag-PSS were prepared by mixing the aqueous solutions of the respective polymers and the colloidal suspension of preformed AgNPs. The coating process of AgNPs by protic polymer PEI and aprotic polymer of PSS were performed by addition of 0.67 mL of each wt.% PEI and PSS to 15 mL of each AgNPs sols making it 20 samples in totals excluding control samples. The solution was stirred continuously during and after addition and it was observed that the shifting of AgNPs sols color takes place within a minute. The yellow-shift occurred for AgNPs/PSS samples after some period of times and the sols shifted to colorless for AgNPs/PEI samples with same procedure as polymer concentration is increased. Thin films of these solutions were casted on glass plates for further analysis especially for Raman and SEM characterisations.

### Kinetic method

To determine the rate of the AgNPs color shifting, the samples were prepared by adding freshly prepared polymer; PEI and PSS at varying concentration to vigorously shaken solutions of AgNPs which contains different colour and size of particles in tube vessels (Fig. 1). The progress of the hue changing was followed through UV-vis spectrum, recording at definite 20 min intervals until 120 min (UV-vis Spectrophotometer-Cary 50) by measuring the absorbance of AgNPs sol formation at range 200-800 nm ( $\lambda_{max}$  of each sol color). The apparent rate constants ( $k_{obs}$ ,  $min^{-1}$ ) were calculated from the initial part of the slopes of the plots of  $\ln(A_0/A_t)$  versus time with a fixed time method (Fig. 5). The pH of the reaction mixture was also measured at the beginning and end of each kinetic experiment.

### Methods of characterization

All the samples products; AgNPs and the AgNPs/polymer complexes were characterized by UV-Vis Spectrometer (Varian Cary 300) with scanning window from 200 to 800 nm band was used. The size distribution of AgNPs in the colloids was measured using a Nano ZS zetasizer system (Malvern Instruments). The chemical bonding and interaction between AgNPs and polymer complexes were analysed using Surface Enhanced Raman Spectroscopy (SERS) and were recorded using Witec Alpha 300R instrument, equipped with the appropriate ( $\times 50$  and  $\times 100$ ) objective lens and 532 nm He-Ne laser with output power up to 70 mW over the range of 3500-400  $cm^{-1}$ . Finally, AgNPs/polymer micrographs were obtained using field emission scanning electron microscopy (FESEM, Inspect FEI F50) and high resolution transmission electron microscopy (HRTEM, 200kV Tecnai G2 20 S-Twin, FEI). The FESEM samples were mounted on the stub and coated with a thin film of 5 nm platinum before observations.

## Results and Discussion:

### General considerations

The first consideration in the preparation of different sized AgNPs is a pH of a reaction mixture because its growth can be controlled by adjusting the pH level of the working solutions. Therefore, control of pH is a crucial problem that we address first by adding sodium borohydride ( $NaBH_4$ ) making it alkaline (pH:  $8.5\pm 0.5$ ) depending on

$NaBH_4$  volume addition. The pH value was found to be nearly constant even with increasing PSS and PEI concentration. Secondly, stability of AgNPs strongly depends on the protective agent that prevents the aggregation of AgNPs. Adsorption of citrate ions on particles surface create a first protective layer that plays a key role in stabilizing growing silver in the working solution. Potassium bromide (KBr) salt was used to shield the negative charges of citrate ions from allowing the particles to clump together with another AgNPs surface and form aggregates. To make sure silver nanoparticles fully stabilized, another surface treatment has been made by using polymers (PEI & PSS) as a layer for AgNPs core to prevent particles from aggregation and functionalised for specific medical application.<sup>17</sup> The nucleated AgNPs/citrate with anionic surface charge is efficiently stabilized against flocculation by the strong coulomb interaction due to the inherent high cationic density of the protic PEI.<sup>18</sup> On the other hand, aprotic PSS with a strong anionic polyelectrolyte, possesses a number of negative charges along its backbone chain which can bind directly towards metallic cations of silver surfaces was used in this experiments as comparison to PEI.<sup>19</sup>

Preliminary observations showed that the reduction of  $Ag^+$  ions with different KBr concentration by fresh borohydride at room temperature turning the colorless mixture to different color as the reaction time increases. Therefore, with different size and color of AgNPs, we choose citrate and polymers as the stabilizing and protecting agents in the present studies. The appearances of different colors were because of different visible light reflectance caused by the surface plasmon resonance of silver nanocrystals in the visible region.<sup>20</sup> The last part of this study is to demonstrate the formation of AgNPs/polymer complexes that could changes or reduces its sols' color at room temperature in a short of time using protic PEI and aprotic PSS. With this goal, a unique adsorption mechanisms between AgNPs and polymers (PEI & PSS) are primarily responsible for the formation of stable AgNPs/polymer in sols and have been observed using Raman spectra (Fig. 7). Extinction and shifting of AgNPs sols color were observed in the range of 0.1, 0.5, 1.0, 1.5 and 2.0 wt.% of PEI and PSS. At higher PSS concentration, the reaction mixture shift to yellow color but in the PEI case, the mixture turns to colorless, because steric stabilization dominates between cationic amine group of PEI and anionic citrate, thus perfectly covering silver surface and neutralised negative charge of citrate on the AgNPs surface.<sup>21</sup> Nevertheless, there is no change in color at low concentration of PSS because of insufficient amount of PSS to cap AgNPs surface as well as replacing citrate shell. Apart from that, precipitates appeared at the bottom of PEI vials samples at a relatively low concentration (0.1 wt.%) because surface coverage was much below the saturation, suspensions may be destabilized due to polymer bridging occurring at this stage.<sup>22,23</sup> Furthermore, different sizes of AgNPs solutions (DLS:  $\sim 2$  &  $\sim 17$  nm) were used to observe the reaction rate of Ag-polymer complexes and as expected, the smaller (yellow sols) shows high reaction rate as the shifting color solutions faster than bigger ones (green sols).

### Effect of the polymer addition

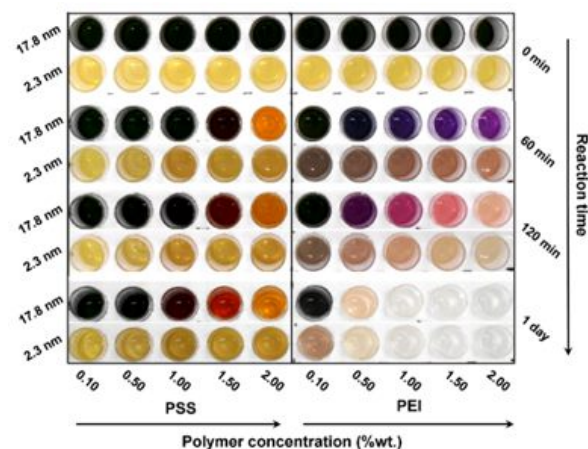


**Figure 1.** Photograph of multicolor AgNPs map obtained as function of variables PSS and PEI at different reaction times.

One of the major findings of the present study was the significant influence of the polymer concentration on the final color of each sample. Due to its functional groups in water solution, the binding of

each functional groups target with AgNPs surface was made possible, forming AgNPs-polymer complexes wherein a replacement or binding together with citrate on AgNPs surface took place.

Moreover, polymers concentration plays a key role for the stabilization of AgNPs along the polymeric chains, controlling their size and shape. In fact, the multicolor AgNPs map illustration in Fig. 1 demonstrates that a sufficiently polymer concentration (0.5-2.0 wt.%), stable AgNPs were generated, showing different sol colors with different reaction time and polymer concentrations.

It is important to remark that 0.1 wt.% PSS shows no color changes even after a week because of low attractive contact strength or surface coverage between AgNPs and PSS, therefore no bound PSS layers form on the AgNPs surface. Conversely, the AgNPs sols colour changes for PEI treatment even 0.1 wt.% but in term of stability, its only stands just for a week depending on AgNPs primary sizes due to polymer bridging between PEI chains.<sup>22</sup>

Those AgNPs with 0.5 to 2.0 wt.% of each polymer showed no changes in the position of their optical absorption bands even after 2 months after completing the reaction and stabilised. Our study demonstrates that by increasing the polymers concentration from 0.1 to 2.0 wt.%, a yellow and colorless-shifted of sols color for AgNPs/PSS and AgNPs/PEI with a variety of hues perceived by the naked eye was obtained with a high stability in time as shown in Fig. 1.

Based on the structural map in Fig. 1, we notice the samples were stable within a specific period and temperatures. The green (AgNPs-1  $\approx$  17 nm) and yellow (AgNPs-2  $\approx$  2 nm) sols are supposed to be in different shapes characterized by vertices which produce wide covering spectra of red and violet wavelength regions, indicating the presence of several surface plasmons of high multipolar order.<sup>16</sup> Contradictorily, the assemblies of AgNPs/polymer relationship are more complex to distinguish because of hydro-dynamically and affinity attraction between functional group of each polymer and AgNPs surface, respectively.

### Characterization of AgNPs/polymers

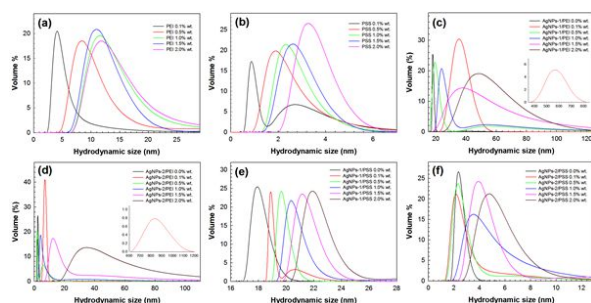


**Figure 2.** DLS size distribution of AgNPs/polymers complexes at 120 min. Control sample: (a) PEI and (b) PSS. From (C) to (F), the final concentration of the polymers (PEI & PSS) was 0, 0.1, 0.5, 1.0, 1.5 and 2.0 wt.% with the different effective particle sizes of AgNPs/PEI and AgNPs/PSS, respectively.

Figure 2 depicts the variation of DLS volume-hydrodynamic size distribution of the AgNPs, polymers (PEI & PSS) and AgNPs/polymers complexes. On top of each graph legends (Fig. 2c-2f) where no addition of polymer at all in the solutions, AgNPs formed which both demonstrated that the effective sizes for AgNPs-1 and AgNPs-2 were formed due to its sol's color.<sup>16</sup> One of the possible reasons for the difference in size of AgNPs produced could be attributed to different concentration of  $\text{NaBH}_4$  interacting with silver precursor, with different nucleation rate according to Lamer and Dinegar model.<sup>24</sup>

The DLS results of the polydispersity of PEI and PSS colloids obtained by mixing monodisperse of both AgNPs-1 and AgNPs-2 are shown in Fig. 2(c-f). According to the DLS spectra, there was a range of nanoparticles present, with hydrodynamic diameters including polymer from about 8 nm to 1.2  $\mu\text{m}$ , assuming a hydration layer of polymer surrounding the AgNPs.

There were also small proportions of aggregates present for 0.1 wt.%

AgNPs/PEI sample as shown in Fig. 2c and 2d (small figure). It is notable that DLS characterization can measure AgNPs sizes including singular and aggregation forms, which is the effective hydrodynamic diameter of AgNPs/polymers complexes rose to larger sizes upon increasing the amount of polymer in the solution, therefore reflecting a wider particle size distribution due to the association of AgNPs with discrete polymer complexes although a minor particle aggregation cannot be ruled out.<sup>25</sup>

A fine control of AgNPs exhibit colorful range depends on the shapes and sizes of the particles and dielectric constant of the surrounding medium due to excitation of surface plasmon resonance band in the visible spectrum, which give rise to such intense colors.<sup>6</sup> As the borohydride solution was mixed with aqueous solution of the silver nitrate and citrate, it started to appear the color due to reduction of silver ion ( $\text{Ag}^+$ ); which indicated the formation of AgNPs.<sup>16</sup> It is generally accepted that UV-vis spectroscopy could be used to examine size and shape-controlled nanoparticles in aqueous solution. Figure 3 shows the UV-Vis spectrum recorded from the reaction medium without polymer concentration and its stable for months.

The absorption spectra of AgNPs sols in Fig. 3 shows two spectral regions consists a single sharp surface plasmon resonance band at 400 nm (region 1: corresponds to spherical shape AgNPs) and broad peak at 700 nm (region 2: corresponds to rod, triangle, or hexagonal shapes AgNPs).<sup>16</sup> Two width regions of this spectrum are due to the presence of more than one SPRs related to transverse and longitudinal electron oscillations.

The most characteristic part of AgNPs sol is a narrow plasmon absorption band observable in the wide range of energy in the range of 350-550 nm regions.<sup>6</sup> The peak appeared at 700 nm band is indicating of new shape forming new localized surface plasmon resonance spectra.<sup>16</sup>

Moreover, the differences in intensity are a consequence of the proportionality of the optical efficiency to the volume of the NP. Besides, size effects also have an influence over the intensity because surface plasmon resonance damping becomes more relevant as electronic surface spill out as the size of the AgNPs becomes small.<sup>26</sup>

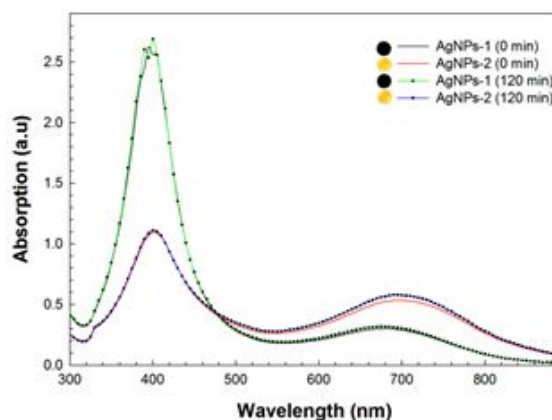


**Figure 3.** UV-vis spectrum of silver nanoparticles absorption with different size and color at 0 and 120 min.

### Effect of [KBr], [PEI] and [PSS] on mechanism of Ag-polymers complexes

The dependence of the AgNPs sols color formation kinetics with the polymer [PEI] and [PSS] were studied between  $0 \leq [\text{PEI} \& \text{PSS}] \leq 2.0$  wt.% at fixed  $[\text{AgNO}_3] = 0.375$  mM,  $[\text{Na}_2\text{CA}] = 12.5$  mM,  $[\text{NaBH}_4] = 5$  mM,  $[\text{H}_2\text{O}_2] = 50$  mM and controlled  $[\text{KBr}] = 1$  mM: 180 & 360  $\mu\text{L}$ . KBr salt with different volumes use to shield or neutralise the negative charge of citrate ions on the AgNPs surface from allowing the particles to clump together to form aggregates. Therefore, increasing the amount of KBr proportionally reduce negative charge of citrate/borohydride ions, and then cause plasmon shift to lower wavelength as the small size of AgNPs (yellow sol) were produced.<sup>27</sup> Fig. 4 shows the UV-Vis spectra for different polymers (PEI & PSS) concentrations, from 0 to 2.0 wt.%, when others reaction condition was kept constant. The absorbance spectra shown in Fig. 4(a & b) suggests that adsorption of PEI on the AgNPs surface results decrease in the

maximum absorption intensity at violet region around 400 nm band and the absorption intensity decreased gradually with time as the PEI concentration was increased due to decreases of surface plasmon resonance.<sup>6</sup> Moreover, the decrease behaviour (hypochromic shift) of absorbance after a definite time interval may be explained in terms of polymer adsorption onto the AgNPs surface. Apart from that, the reduction absorbance-[AgNPs] shows proportional dependence of the silver sol interaction with PEI resulting in colorless sols after periods of time depending on PEI concentration. Moreover, citrate-capped AgNPs with negative charge were brought in contact with cationic aqueous PEI, forming thick layer around AgNPs core. Also, the scattering from thick PEI shell would screen the surface and as the results the plasmon resonance does not occur. Thus, we concluded that the PEI sealed off AgNPs surface, thus reducing its surface plasmon resonance.

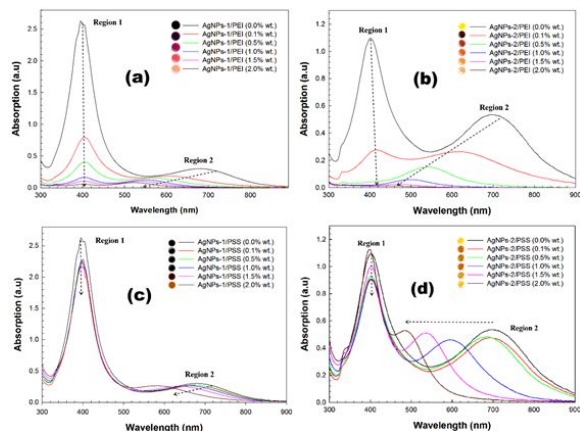


**Figure 4.** Evolution of UV-vis absorption spectra of AgNPs sols with different [PEI & PSS] weight concentrations; (a) AgNPs 1-PEI, (b) AgNPs 2-PEI, (c) AgNPs 1-PSS and (d) AgNPs 2-PSS sols formation at 120 min after polymers addition (AgNPs sols photograph can refer the AgNPs multicolor map at Fig. 1).

Figure 4(c & d) was also plotted to show a clearer picture of the evolution of optical absorption bands (regions 1 & 2) when the concentration of PSS was increased. An absorption band located at red region (region 2: 600-700 nm) of Fig. 4(d) with small size of AgNPs obviously shifts to violet wavelength (400 nm) and slightly decrease its intensity peak in region 1 (violet region) as the PSS concentration is increased compared to bigger size of AgNPs (Fig. 4c) with the resulting yellow color indicates the excitation of the LSPR of spherical shapes and well dispersed in the solution due to the dielectric properties of the surrounding environment changed.<sup>25</sup>

Another reason is PSS with strong anionic sulfonate functional group could replace citrate ions and attracted electrostatically towards AgNPs surface due to high affinity compared to citrate, resulting in greater charge neutralization of AgNPs surface and produces stronger van der Waals force between AgNPs/PSS.<sup>25</sup> In addition, when the PSS weight concentration is increased, the generation of new colors is achieved (Fig. 4c-d) with yellow-shift of sols color (Fig. 1).

These changes in sols color from green (AgNPs-1) and bright yellow (AgNPs-2) to dark yellow (higher PSS concentration) in all samples including AgNPs-1 and AgNPs-2 can be perfectly controlled during the synthesis process as a function of PSS added in the initial solution.

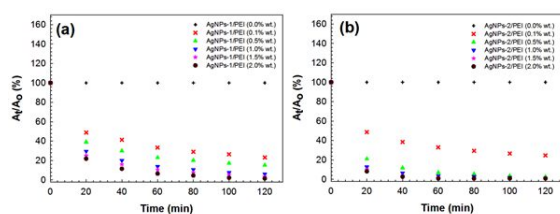


**Figure 5.** Effects of PEI on the surface plasmon absorbance at 400 nm of

(a) AgNPs-1 and (b) AgNPs-2 sols formation at different time intervals.

Reaction conditions: [+] = 0.0 wt.% PEI, [x] = 0.1 wt.% PEI, [▲] = 0.5 wt.% PEI, [▼] = 1.0 wt.% PEI, [⊠] = 1.5 wt.% PEI and [●] = 2.0 wt.% PEI.

The effect of PEI concentrations was further studied in order to understand the colour extinction of silver sols due to adsorption onto its surface. The observed results are depicted in Fig. 5 as percentage reduction of absorbance AgNPs/PEI's series. From the reduction curve, there is only slight decrease to 75% for AgNPs-1/PEI compared to 77% for AgNPs-2/PEI of 0.1 wt.% PEI but shows 99% of reduction for both at 2.0 wt.% from maximum absorption after chemical reaction for 120 min.

Apart from the graphs, the curves clearly demonstrate that AgNPs-2/PEI exhibit better reduction of absorbance peaks compared to AgNPs-1/PEI curves, respectively. Lower reaction rate of AgNPs-1/PEI may be attributed to bigger particles size compared to AgNPs-2/PEI that might need more time to seal AgNPs surface.

Furthermore, with increasing PEI concentration in solution, the reaction rate and colour extinction would increase spontaneously as shown in Fig. 5. All these considerations, along with the above observed results, lead to the proposal of the following mechanism for the extinction of AgNPs sols colour as shown in Fig. 6.

### Role of polymers and reaction site to the growth of Ag-nanocrystals

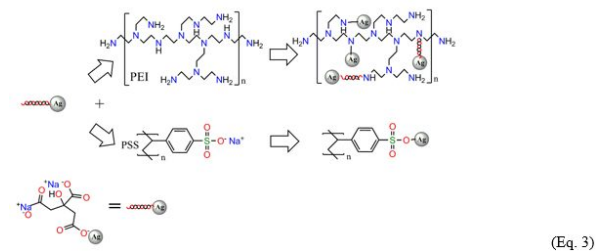
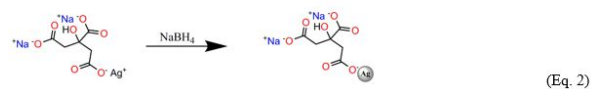
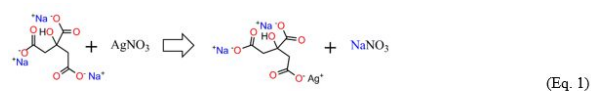


**Figure 6.** Schematic illustration for AgNPs/PEI's and AgNPs/PSS's complexes.

Polymers can stabilize the particles through electrostatic forces,<sup>29</sup> hydrogen bonding<sup>30</sup> and van der Waals forces<sup>31</sup> between functional groups and inorganic particles. Thus, various properties such as oxidation-reduction potentials,<sup>32</sup> quantum efficiencies,<sup>33</sup> reaction mechanisms,<sup>29</sup> size,<sup>6</sup> and shape<sup>16</sup> of inorganic chemicals are changed in the presence of polymers. In the present study, role of polymers (PEI & PSS) could be explained by incorporation of polymers onto the surface of AgNPs through schematic in Fig. 6. Equation 1 represents the formation of Ag<sup>-</sup>citrate complexes by silver nitrate and trisodium citrate reaction. In the second reaction (Eq. 2), with controlling pH level in the solution by NaBH<sub>4</sub> making Ag<sup>+</sup>-citrate complex decomposes in one step one-electron oxidation reduction mechanism to produces AgNPs/citrate and shield the AgNPs surfaces.

In the final step, the polymerization of the formed AgNPs/polymer complexes with PEI and PSS occurred by replacing or binding together with citrate shell and seal onto AgNPs surfaces (Eq. 3). The sulfonate group of PSS adsorbs onto AgNPs surface via electrostatic interaction of R-COO<sup>-</sup>/Ag<sup>+</sup> resulting yellow-shift in RCOO<sup>-</sup>-AgNPs sols colour (Fig. 8b). Apart from that, amine groups in PEI chains have strong tendency to coordinate with AgNPs or AgNPs-citrate forming AgNPs/PEI or AgNPs/citrate/PEI complexes. Therefore, AgNPs

attached at primary and secondary amine groups of PEI through protonated process as shown in Eq. 3. The sols color was turning to colorless once the reaction between AgNPs or AgNPs-citrate and PEI functional groups completed. The proposed mechanism is further supported by the Raman spectrums in Fig 9.

Basically, the key material parameter in hue change is the polymer segment and AgNPs attractive contact strength, the absolute value of which controls the aggregation state. There are three levels of the polymer segment and nanoparticles attractive contact between AgNPs and polymer; at low attractive contact strength values or surface coverage is much below the saturation, suspensions would be destabilized due to polymer bridging and depletion attractions making AgNPs aggregate into compact clusters, therefore thin layer of sediment appeared at the bottom of vials.<sup>34</sup>

At the intermediate interfacial cohesion strength, a net repulsive interparticle potential of mean force (PMF) between the AgNPs and polymer produces thermodynamically stable "bound polymer layers" form around nanoparticles, making it stable and fully dispersed at all particle volume fractions.<sup>34</sup> At the large values, polymers form tight bridges between the AgNPs, resulting in phase separation or perhaps formation of non-equilibrium polymer particle networks.<sup>34</sup> Therefore, in our experimental system, there is favourable adsorption energy for polymers on AgNPs surfaces as PEI and PSS adsorbs to the AgNPs surfaces proportional to polymers concentration as the polymer-particle attraction strength in low concentration is much weaker than in high polymer concentration.

SEM studies were performed to confirm further the AgNPs in the polymer, as shown in Fig. 7(a-d). It is interesting to note that the hydrodynamic diameters of AgNPs in the presence of PEI and PSS measured by dynamic light scattering (DLS) experiments were much smaller than the SEM measured diameters of AgNPs/polymer, indicating the formation of a much bigger volume of PEI & PSS-involved assembly structures and many monodispersed AgNPs were contained in such AgNPs/polymers assembly structures. Therefore, the arrangement of AgNPs in the polymer layer next will be confirming using micrographs of HRTEM as shown in Fig. 8.

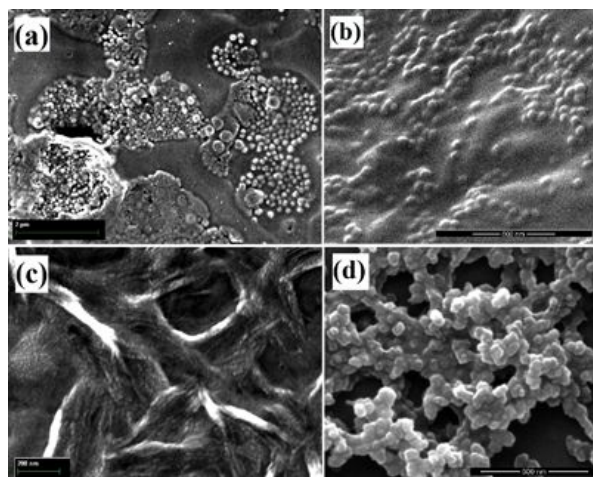


**Figure 7.** SEM micrographs that show the formation of AgNPs/polymer's complexes with different AgNPs sizes and 2.0% wt. of polymer concentration:

- (a) AgNPs-1/PEI,
- (b) AgNPs-2/PEI,
- (c) AgNPs-1/PSS and
- (d) AgNPs-2/PSS.

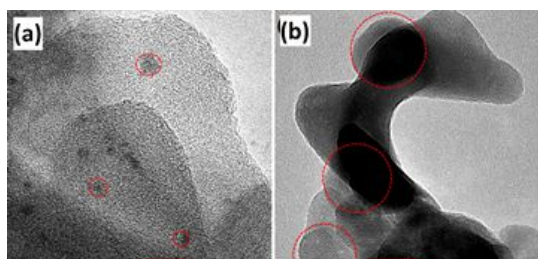


**Figure 8.** HRTEM micrographs that show the selected formation of AgNPs/polymer's complexes with different AgNPs sizes and 2.0% wt. of polymer concentration:

- (a) AgNPs-2/PEI and
- (b) AgNPs-1/PSS.

HRTEM micrographs were performed to further investigate the AgNPs in the polymer, as shown in Fig. 8a and 8b. Here, the diameters of AgNPs-1 and AgNPs-2 in the presence of PEI and PSS shows the same scale with measured by dynamic light scattering (DLS), indicating of the single AgNPs measurement. Furthermore, the reason for the gradual absence of absorbance peaks of AgNPs/PEI's series in Fig. 5 could be explain due to adsorption of thick PEI layer onto its surface as shown in Fig. 8a. Meanwhile, strong van der Waals forces between AgNPs surface and PSS functional group resulting the particles packed close to each other as shown in Fig. 8b.

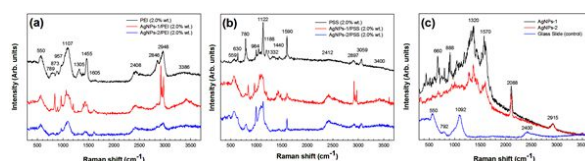


**Figure 9.** SERS spectra with 532 nm laser excitation for (a) AgNPs/PEI, (b) AgNPs/PSS and (c) AgNPs & Borosilicate glass slide (control).

Figure 9 shows the SERS spectra of the polymer adsorbed on AgNPs surface acquired using a 532-nm laser. The SERS spectrum for single PEI 2.0 wt.% (Fig. 8a: black line) shows an intense band at  $1455\text{ cm}^{-1}$  that is clearly attributed to  $\delta(\text{CH}_2)\text{-}\delta(\text{CH}_2)$  asymmetry bending. Other bands appearing at  $1305$ ,  $1107$ , and  $957\text{ cm}^{-1}$  are also attributed to methylene groups, in particular to  $\text{CH}_2$  wagging and twisting motions, because these bands are also found in Raman spectra of polyethylene<sup>35</sup> and ethylene diamine.<sup>36</sup> The band of  $\text{CH}_2$  appears at  $1035\text{ cm}^{-1}$  in the top spectra of Figure 9a undergoes flat when the polymer is adsorbed on the AgNPs surface due to aliphatic moieties.<sup>37</sup> In particular, the band at  $550\text{ cm}^{-1}$  can be attributed to the C-N bond, which together with the  $1107\text{ cm}^{-1}$  band intercepted with borosilicate glass slide of  $\nu(\text{Si-O-Si})$  band (see Fig. 9c), making it one of higher intensity peaks in the spectrum. The weak bands observed at  $789\text{-}873$  and  $1605\text{ cm}^{-1}$  appear due to the rocking vibrations of ethylene groups and the amine bending ( $\delta(\text{NH}_2)$ ) from the PEI chains.<sup>37</sup> The weak band appeared at  $3386\text{ cm}^{-1}$  assigned to N-H stretch vibration of PEI demonstrated that PEI was successfully grafted to AgNPs surface. However, the adsorption of PEI on AgNPs surface could create the formation of a Lewis acid-base interaction between the amine groups and the AgNPs metal, thus leading to a marked change in the Raman spectrum.<sup>37</sup> The asymmetric ( $\nu_{\text{as}}$ ) and symmetric ( $\nu_{\text{s}}$ ) stretching motions of C-H bands are slightly shifted up and downwards in AgNPs/PEI spectrum due to the presence of amino groups in its complexes structure (Fig. 6). These modes appear at  $2846$  and  $2954\text{ cm}^{-1}$  shifted when the polymer is adsorbed on the AgNPs's surface. Furthermore, the shift of the amino band between  $1400$  and  $1610\text{ cm}^{-1}$  in the spectrum suggests a change in the protonation state of these groups as a consequence of the interaction with the AgNPs surface, indicating that an aminolysis reaction or an electrostatic interaction had taken place between both sides.<sup>37</sup> Moreover, the above bands may also due to  $\delta(\text{NH}_2^+)$  in protonated secondary amines or  $\delta(\text{NH}^+)$  in protonated tertiary amines.<sup>38</sup>

This interaction mechanism is the most probable one taking into account that the residual charge of the AgNPs surface is negative as treated with citrate and the positive charge of the PEI is localized on the amino groups. The band shifts observed at the spectra suggest the existence of different amino groups (primary, secondary, and tertiary) of PEI on the AgNPs surface could be either adsorbed onto the AgNPs surface forming ionic pair (through electrostatic interaction with negative charges existing on the surface together with citrate or a coordination complex direct with the AgNPs surface) or surrounded by aliphatic groups with a different conformation.<sup>39,40</sup> The amide bond linking the citrate to PEI generally comes in the near region of  $1605\text{ cm}^{-1}$  as shown in Fig. 9a (AgNPs 1-red line) attributed to  $\text{COO}^-$  Ag vibrations. In the present spectrum, it appears to be overlapped with the N-H bending mode as the number of amines is comparatively higher in the compound. Thus, the reason why the AgNPs-PEI solution couldn't hold the sols color is because of interaction between citrate and amine group of PEI.

Figure 9(b) is the prominent SERS spectrum of AgNPs and PSS 2.0 t.%, with two sharp bands at 1122 and 1590  $\text{cm}^{-1}$  corresponding to  $\nu(\text{C}-\text{C})$  aliphatic chain and  $\nu(\text{C}=\text{C})$  vibrations of aromatic ring, could be clearly observed in the PSS spectrum attributed to molecular benzene, respectively.<sup>41</sup> Other than that, the bands at 2897 and 3059  $\text{cm}^{-1}$  also attributed to benzene ring due to  $\nu(\text{C}-\text{H})$  and  $\nu(=\text{C}-\text{H})$  vibrations, respectively.<sup>42</sup> Other bands appearing at 630 and 780  $\text{cm}^{-1}$  are attributed to  $\nu(\text{C}-\text{S})$  aliphatic vibrations due to sulfonate functional group.<sup>43</sup> Moreover, the band at 1100  $\text{cm}^{-1}$  was corresponding to  $\nu(\text{C}-\text{S})$  aromatic vibrations also found in the spectrum.<sup>43</sup> The peak at 1440  $\text{cm}^{-1}$  can be assigned to  $\text{C}_a=\text{C}_p$  symmetric vibrations and 1332  $\text{cm}^{-1}$  to C-C stretching deformations of PSS.<sup>43</sup> At the same concentration, some features of PSS are underneath the major peaks of AgNPs/PSS. These SERS peaks of AgNPs/PSS broadening agree well with the result of AgNPs and adsorbed PSS coexistence (red & blue lines).

In contrast, the SERS intensity spectrum obtained for both AgNPs (Fig. 9(c)) are quite high due to resonance effect induced by a possible charge transfer attribute to the interaction of citrate ions with the AgNPs surface.<sup>44</sup> The existence of a charge transfer was responsible for the resonant effect observed on Fig. 9(a & b) as the intensity peaks reduced in the spectra is additional proof demonstrating the establishment of a strong interaction between amine groups (PEI) and sulfonate group (PSS) with the AgNPs and thick layer of both shell leading to a change in the PEI protonation state and functionalised sulfonate groups for PSS. Apart from that, AgNPs structural marker bands mainly appear at 450 and 1570  $\text{cm}^{-1}$  attributed to  $\nu(\text{Ag}-\text{O})$  and  $\text{COO}-\text{Ag}$  vibrations.<sup>45</sup> The band features at 2088  $\text{cm}^{-1}$  was attributed to the  $\nu(\text{C}-\text{N})$  symmetric stretches shifted to lower wavenumbers that corresponded to -NO<sub>2</sub> functional group.<sup>37</sup> The principal band is at 1320  $\text{cm}^{-1}$ , which is assigned as the carboxylate symmetric stretching mode from citrate,  $\nu_s(\text{COO})$ .<sup>45,46</sup> When compared with the Raman spectrum of trisodium citrate in solution (~1417  $\text{cm}^{-1}$ ), this band is broadened and blue-shifted, indicating interactions between the carboxylates and the AgNPs surface.<sup>45</sup> This is also supported by the decreasing of the bands at 1291 and 1243  $\text{cm}^{-1}$  which are associated with the carboxylate deformations,  $\delta(\text{COO})$ .<sup>46</sup> The bands at 888  $\text{cm}^{-1}$  are assigned to the  $\nu(\text{C}-\text{C})$  aliphatic chain and  $\nu(\text{C}-\text{O}-\text{C})$  symmetry vibrations modes also from citrate. Moreover, the peaks in the 2830-3000  $\text{cm}^{-1}$  regions are attributed to the symmetric and asymmetric C-H stretching modes of the -CH<sub>2</sub> and -CH<sub>3</sub> groups.<sup>37</sup> Apart from that, the band appear at 660  $\text{cm}^{-1}$  (AgNPs I-Black line) due to  $\nu(\text{C}-\text{Br})$  vibration modes, which is ionic bromine from KBr interact with citrate at the same point as well.<sup>47</sup>

## Conclusions:

In summary, we have successfully synthesized and observed a hue changing of AgNPs sols as a function of variable PEI and PSS concentrations with a constant concentration of silver precursor using a chemical reduction method. It has been demonstrated that a fine control of both PEI and PSS concentrations in different sizes of AgNPs made it possible to changes or reduces its color due to interaction between AgNPs and specific polymer functional groups. Thus, the reaction sols of AgNPs shift to yellow and colorless quickly at higher polymers concentration. Additionally, the rate of color shifting also depends on concentration levels of polymers addition. Based on the comprehensive SERS experiments, it is concluded that the existence of different amino groups of PEI adsorbed onto AgNPs surface either by interaction with citrate that react as a linker between AgNPs and PEI or a coordination complex direct with the AgNPs surface. In contrast, the SERS peaks of AgNPs/PSS broadening around sulfonate group agree well with the result of adsorbed PSS onto the AgNPs surfaces. SERS results were supported by absorbance spectra, which suggest that adsorption of PEI and PSS on the AgNPs surface results decrease in the maximum absorption intensity at violet region due to decreases of surface plasmon resonance, resulting colorless and yellow sols of both AgNPs/PEI and AgNPs/PSS at the end of experiments.

## Acknowledgements:

This work has been supported by Flinders University, Australia and The National University of Malaysia (UKM), Malaysia through an equal contribution of Cotutelle Programme. Additional sources of funding from UKM's grant (Ap-2015-006).

## References:

1. I. Pantic, *Rev. Adv. Mater. Sci.*, 2014, 37, 15.
2. Y. Zhang, R. Huang, X. F. Zhu, L. Z. Wang and C. X. Wu, *Rev. Mater. Sci.*, 2012, 57, 238.
3. N. Kalfagiannis, P. G. Karagiannidis, C. Pitsalidis, N. T. Panagiotopoulos, C. Gravalidis, S. Kassavetis, P. Patsalas and S. Logothetidis, *Solar Energy Materials and Solar Cells.*, 2012, 104, 165.

4. W. H. D. Jong and P. J. Borm, *Int. J. Nanomedicine.*, 2008, 3, 133.
5. A. D. McFarland and R. P. Van Duyne, *Nano Letters.*, 2003, 3, 1057.
6. A. L. Gonzalez, C. Noguez, J. Beranek and A. S. Barnard, *J. Phys. Chem. C.*, 2014, 118, 9128.
7. Z. Huang, X. Jiang, D. Guo and N. Gu, *J. Nanosci Nanotechnol.*, 2011, 11, 9395.
8. H. Liu, H. Wang, R. Guo, X. Cao, J. Zhao, Y. Luo, M. Shen, G. Zhang and X. Shi, *Polym. Chem.*, 2010, 1, 1677.
9. L. Gutierrez, C. Aubry, M. Cornejo and J. P. Croue, *Langmuir.*, 2015, 31, 8865.
10. Z. Chen, X. Zhang, H. Cao and Y. Huang, *Analyst.*, 2013, 138, 2343.
11. S. Agnihotri, S. Mukherji and S. Mukherji, *Nanoscale.*, 2013, 5, 7328.
12. G. F. Prozorova, A. S. Pozdnyakov, N. P. Kuznetsova, S. A. Korzhova, A. I. Emel'yanov, T. G. Ermakova, T. V. Fadeeva and L. M. Sosedova, *Int. J. Nanomedicine.*, 2014, 9, 1883.
13. N. Beyth, Y. Hourri-Haddad, L. Baraness-Hadar, I. Yudovin-Farber, A. J. Domb and E. I. Weiss, *Biomaterials.*, 2008, 29, 4157.
14. B. C. Herold, N. Bourne, D. Marcellino, R. Kirkpatrick, D. M. Strauss, L. J. Zaneveld, D. P. Waller, R. A. Anderson, C. J. Chany, B. J. Barham, L. R. Stanberry and M. D. Cooper, *J. Infect Dis.*, 2000, 181, 770.
15. Y. S. Ye, J. Rick and B. J. Hwang, *Polymers.*, 2012, 4, 913.
16. P. J. Rivero, J. Goicoechea, A. Urrutia and F. J. Arregui, *Nanoscale Research Letters.*, 2013, 8, 101.
17. S. Y. Kim and C. F. Zukoski, *Langmuir.*, 2011, 27, 10455.
18. N. G. Bastus, F. Merkoci, J. Piella and V. Puntes, *Chem. Mater.*, 2014, 26, 2836.
19. N. Zhang, X. Yu, J. Hu, F. Xue and E. Ding, *RSC Adv.*, 2013, 3, 13740.
20. J. Wei, N. Schaeffer, P. A. Albouy and M. P. Pileni, *Chem. Mater.*, 2013, 27, 5614.
21. G. F. Fritz, V. Scha'dler, N. Willenbacher and N. J. Wagner, *Langmuir.*, 2002, 18, 6381.
22. J. Swenson, M. V. Smalley and H. L. M. Hatharasinghe, *Phys. Rev. Lett.*, 1998, 81, 5840.
23. V. Runkana, P. Somasundaran and P. K. Kapur, *Chemical Engineering Science.*, 2006, 61, 182.
24. V. K. LaMer, R. H. Dinegar, *J. Am. Chem. Soc.*, 1950, 72, 4847.
25. J. K. Lim, S. P. Yeap, H. X. Che and S. C. Low, *Nanoscale Research Letters.*, 2013, 8, 381.
26. Jean Lerm, *J. Phys. Chem. C.*, 2011, 115, 14098.
27. N. Cathcart, A. J. Frank and Vladimir Kitaev, *Chem. Commun.*, 2009, 46, 7170.
28. R. A. Sperling, W. J. Parak, *Phil. Trans. R. Soc. A.*, 2010, 368, 1333.
29. E. A. Appel, M. W. Tibbitt, J. M. Greer, O. S. Fenton, K. Kreuels, D. G. Anderson and R. Langer, *ACS Macro Lett.*, 2015, 4, 848.
30. K. Heo, C. Miesch, T. Emrick and R. C. Hayward, *Nano Lett.*, 2013, 13, 5297.
31. G. A. Rance, D. H. Marsh, S. J. Bourne, T. J. Reade and A. N. Khlobystov, *ACS Nano.*, 2010, 4, 4920.
32. O. S. Ivanova and F. P. Zamborini, *J. Am. Chem. Soc.*, 2010, 132, 70.
33. L. W. Jang, D. W. Jeon, T. Sahoo, D. S. Jo, J. W. Ju, S. J. Lee, J. H. Baek, J. K. Yang, J. H. Song, A. Y. Polyakov and I. H. Lee, *Optics Express.*, 2012, 20, 2116-2123.
34. Y. N. Pandey, G. J. Papakonstantopoulos and M. Doxastakis, *Macromolecules.*, 2013, 46, 5097.
35. P. J. Hendra and J. K. Agbenyega, *John Wiley & Sons: Chichester*, 1993
36. Bruker Analytische Messtechnik GmbH library, 1995
37. S. S. Cortes, R. M. Berenguel, A. Madejon and M. P. Me'ndez, *Biomacromolecules.*, 2002, 3, 655.
38. N. B. Colthup, L. H. Daly and S. E. Wiberly, *Academic Press: New York*, 1975.
39. S. K. Sun, H. F. Wang and X. P. Yan, *Chem. Commun.*, 2011, 47, 3817
40. S. Chakraborti, P. Joshi, D. Chakravarty, V. Shanker, Z. A. Ansari, S. P. Singh and P. Chakraborti, *Langmuir.*, 2012, 28, 11142.
41. Y. J. Liu, Z. Y. Zhang, R. A. Dluhy and Y. P. Zhao, *J. Raman Spectrosc.*, 2010, 41, 1112.
42. X. Ren, E. Tan, X. Lang, T. You, L. Jiang, H. Zhang, P. Yin, and L. Guo, *Phys. Chem. Chem. Phys.*, 2013, 15, 14196.
43. M. S. Barba and A. M. Kelley, *J. Phys. Chem. C.*, 2010, 114, 6822.
44. S. Sakamoto, M. Okumura, Z. Zhao and Y. Furukawa, *Chemical Physics Letters.*, 2005, 412, 395.
45. S. Pattanayak, A. Swarnkar, A. Priyam and G. M. Bhalerao, *Dalton Trans.*, 2014, 43, 11826.
46. Y. Zhang, F. Wang, H. Yin and M. Hong, *Advances in Nanoparticles.*, 2013, 2, 104.
47. G. Socrates, *John Wiley & Sons*, 2004, 206.